Journal of proteome research

Article

pubs.acs.org/jpr

Integrating Proteomics and Enzyme Kinetics Reveals Tissue-Specific Types of the Glycolytic and Gluconeogenic Pathways

Jacek R. Wiśniewski,*,† Agnieszka Gizak,‡ and Dariusz Rakus‡

†Biochemical Proteomics Group, Department of Proteomics and Signal Transduction, Max-Planck-Institute of Biochemistry, D-82152 Martinsried, Germany

‡Department of Animal Molecular Physiology, Wroclaw University, PL-50205 Wroclaw, Poland

Supporting Information

ABSTRACT: Glycolysis is the core metabolic pathway supplying energy to cells. Whereas the vast majority of studies focus on specific aspects of the process, global analyses characterizing simultaneously all enzymes involved in the process are scarce. Here, we demonstrate that quantitative label- and standard-free proteomics allows accurate determination of titers of metabolic enzymes and enables simultaneous measurements of titers and maximal enzymatic activities (A_{max}) of all glycolytic enzymes and the gluconeogenic fructose 1,6-bisphosphatase in mouse brain, liver and muscle. Despite occurrence of tissue-specific isoenzymes bearing different kinetic properties, the enzyme titers often correlated well with the A_{max} values. To provide a more general picture of energy metabolism, we analyzed titers of the enzymes in additional 7 mouse organs and in human cells. Across the analyzed samples, we identified two basic profiles: a "fast glucose uptake" one in brain and heart, and a "gluconeogenic rich" one occurring in liver. In skeletal muscles and other organs, we found intermediate profiles. Obtained data highlighted the glucose-flux-limiting role of hexokinase which activity was always 10- to 100-fold lower than the average activity of all other glycolytic enzymes. A parallel determination of enzyme titers and maximal enzymatic activities allowed determination of k_{cat} values without enzyme purification. Results of our in-depth proteomic analysis of the mouse organs did not support the concepts of regulation of glycolysis by lysine acetylation.

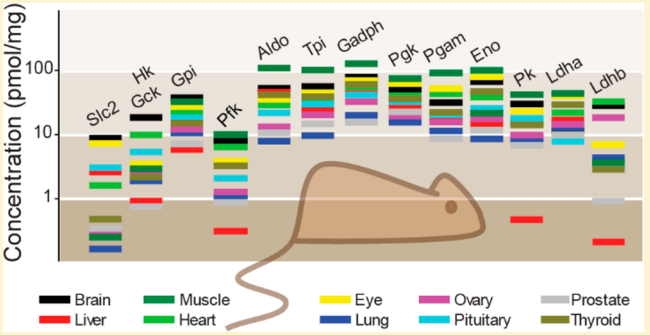

KEYWORDS: *glycolysis, gluconeogenesis, carbohydrate metabolism, energy metabolism, quantitative proteomics, "total protein approach", "filter aided sample preparation" absolute protein quantitation, lysine acetylation, k_{cat}-values*

INTRODUCTION

Glycolysis is one of the basic metabolic pathways supplying the cell with energy and, at the same time, with the material for a variety of syntheses. Enzymatically catalyzed glycolytic reactions take place in every cell, from microorganisms to man.[1] Glycolysis has been extensively studied over several decades. Despite this, recent investigations provide novel insights in the regulation of the glycolytic pathway. These include analysis of posttranslational processes such as the acetylation of glycolytic enzymes,[2,3] and elucidation of discrete roles of isoenzymes such as the role of pyruvate kinase M2 in promotion of the Warburg effect.[4,5]

Characterization of the metabolic capacity of individual enzymes as well as studying these enzymes in context of a metabolic pathway usually requires determination of the enzyme concentrations. Over the last three decades, for unpurified proteins, this task was most frequently conducted using Western blotting. Although this technique is proven, it requires specific antibodies which sometimes are not available. Recent proteomic studies bypassed these analytical constraints by applying "targeted proteomics" approaches to study metabolic pathways including glycolysis.[6−8] These methods allowed quantitation of larger numbers of enzymes using stable-isotope-labeled standards, and required preselection of targeted peptides for monitoring of a given reaction.

Here, we applied the recently developed and validated label- and standard-free proteomic approach[9−11] to characterize glycolysis and gluconeogenesis by providing quantitative protein data for each enzyme across different mouse tissues and human cells. We integrated these data with enzymatic measurements, providing systems-wide insights in the organization of basic metabolic pathways.

We demonstrate that the abundance values can often be used as the proxy for total enzymatic activity. Our results highlight the role of hexokinase as the major rate-limiting enzyme in glycolysis. Relative to other glycolytic enzymes, hexokinases are more abundant in brain and heart, whereas in skeletal muscles, their levels are 1−2 orders of magnitude lower. Low levels of phosphofructokinase and pyruvate kinase, which are commonly considered as regulatory enzymes of glycolysis, were found only in liver, the organ with extensive gluconeogenesis.

Received: March 31, 2015
Published: June 16, 2015

DOI: 10.1021/acs.jproteome.5b00276
J. Proteome Res. 2015, 14, 3263−3273

EXPERIMENTAL PROCEDURES

Mouse Tissue Lysis

Freshly dissected tissues from adult Swiss white mice were homogenized with Ultra Turrax T8 homogenizer (IKA Labortechnik) in ice-cold buffer: 20 mM Tris-HCl, 1 mM EDTA, 1 mM EGTA, 1 mM DTT, 60 mM NaF, 1 mM PMFS, 1 g/mL leupeptin, pH 7.4, 4 °C. For the proteomic analysis, protein extracts were supplemented with SDS and DTT to final concentrations of 2% and 0.05 M, respectively. The lysis was completed by incubations of the mixtures at 100 °C, for 5 min.

Enzyme Assays

Enzyme activities were assayed using cytosolic fractions of mouse brain, liver and skeletal muscle, obtained by centrifugation of the homogenate (see above) at 20 000*g*, at 4 °C, for 20 min. An enzyme activity, expressed in U [mol min^{-1}] was determined from the difference in the slope of NAD(P)H absorbance (340 nm; ε = 6.22 mM^{-1} cm^{-1}) before and after addition of a substrate. The activities, unless stated otherwise, were measured in 50 mM BisTrisPropanol buffers with 150 mM KCl, 0.25 mM EDTA and 5.25 mM $MgCl_2$, pH 7.4, 37 °C based on the assays described by Teusink et al.[12] The contents of the reaction mixtures (V =1 mL) were as follows: the hexokinase (HK) reaction mixture contained 1 mM ATP, 0.4 mM NADP, 5 units glucose-6-phosphate dehydrogenase (G6PDH) and 100 mM glucose as the substrate. Total $MgCl_2$ concentration was 15.25 mM. The phosphoglucose isomerase (PGI) reaction mixture contained 0.4 mM NADP, 2 units G6PDH and 10−20 mM fructose-6-phosphate (F6P) as the substrate. The phosphofructokinase (PFK) reaction mixture contained 0.01 mM fructose-2,6-bisphosphate, 0.2 mM NADH, 1 mM F6P, 5 units glycerol-3-phosphate dehydrogenase (G3PDH), 5 units aldolase and 5 U triosephosphate isomerase (TPI), 3 mM DTT, 0.02 mM AMP and 1 mM ATP; KCl concentration was 100 mM. The aldolase reaction mixture contained 0.2 mM NADH, 5 units G3PDH, 5 units TPI and 0.5 mM fructose-1,6-bisphosphate (F1,6P2). The TPI reaction mixture contained 1 mM NAD^+, 10 mM disodium hydrogen arsenate, 5 U glyceraldehyde-3-phosphate dehydrogenase (GAPDH) and 10 mM Li-dihydroxyacetone phosphate. The glyceraldehyde-3-phosphate dehydrogenase reaction mixture contained 1 mM NAD^+, 20 U TPI, 50 mM disodium hydrogen arsenate, 2.4 mM glutathione and 10 mM Li-dihydroxyacetone phosphate. The reaction was carried out in 50 mM trietanolamine buffer, pH 7.4, 37 °C. The phosphoglycerate kinase reaction mixture contained 0.2 mM NADH, 1 mM ATP, 5 units GAPDH and 5 mM 3-phosphoglycerate; $MgCl_2$ concentration was 10.25 mM, and instead of KCl, 100 mM NaCl was used in a buffer. The phosphoglycerate mutase reaction mixture contained 0.2 mM NADH, 1 mM 2,3-bisphosphoglycerate, 1.5 mM ADP, 2.5 units lactate dehydrogenase,[13] 2.5 units pyruvate kinase (PK), 2.5 units enolase and 10 mM 3-phosphoglycerate (3PG); $MgCl_2$ concentration was 10.25 mM and 100 mM NaCl was used in a buffer instead of KCl. The enolase reaction mixture contained 0.2 mM NADH, 1.5 mM ADP, 2.5 units LDH, 2.5 units PK and 2 mM 2-phosphoglycerate as the substrate; $MgCl_2$ concentration was 10.25 mM and 100 mM NaCl was used in a buffer instead of KCl. The pyruvate kinase reaction mixture contained 0.2 mM NADH, 5 mM phosphoenolpyruvate, 3 mM DTT, 0.1 mM F1,6P2, 2.5 units LDH and 1.5 mM ADP. The lactate dehydrogenase reaction mixture contained 0.2 mM NADH and 2 mM pyruvate; $MgCl_2$ concentration was 10.25 mM and 100 mM NaCl was used in a buffer instead of KCl. The fructose 1,6-bisphosphatase (FBP) reaction mixture contained 0.2 mM NADP, 2 units G6PDH, 2 units PGI and 0.2 mM F1,6P2.

Purification of Aldolase

Aldolase from C57BL/6 mouse liver and skeletal muscles was purified according to Penhoet et al.[14] At each step of the purification aliquots were taken, assayed for aldolase activity, and lysed in the SDS-containing buffer (see above) for proteomic analysis and SDS-PAGE.

Protein Digestion and Peptide Fractionation

Protein lysates and extracts containing 100 μg of total protein were processed in the 30k filtration units (Cat No. MRCF0R030, Millipore)[15] using the MED-FASP protocol.[16] Endoproteinase Lys-C and trypsin were used for sequential digestion of proteins. The enzyme to protein ratios were 1/50. Triplicates of each sample were prepared and analyzed.

Determination of Total Protein and Peptide

Protein and peptide concentrations were assayed using the tryptophan fluorescence assay as described recently.[17]

Western Blot Analysis

The lysates of muscle samples were electrophoresed, transferred to nitrocellulose, and probed as described previously.[18] Briefly, aliquots of whole tissue lysates containing 17, 5, 1.7, 0.5, and 0.15 μg of total protein were separated on SDS gels and were blotted onto nitrocellulose. After protein fixation with 0.5% glutaraldehyde, the blots were stained with Ponceau S to test the quality of the protein transfer. Antibodies against mouse HK1 and HK2 were from Millipore/Chemicom, whereas antibodies against aldolase, fructose 1,6-bisphosphatase, muscle pyruvate kinase, and phosphoglicerate kinase were produced and purified as described previously.[19]

LC−MS/MS Analysis

Analysis of the peptide mixtures was performed using HCD fragmentation mode as described previously.[20] Briefly, the peptides were separated on a reverse phase column (20 cm × 75 μm inner diameter) packed with 1.8 μm C18 particles (Dr. Maisch GmbH, Ammerbuch-Entringen, Germany) using a 4 h acetonitrile gradient in 0.1% formic acid at a flow rate of 250 nL/min. The LC was coupled to a Q Exactive mass spectrometer (Thermo Fisher Scientific, Germany) via a nanoelectrospray source (Proxeon Biosystems, now Thermo Fisher Scientific). The Q Exactive was operated in data dependent mode with survey scans acquired at a resolution of 50 000 at m/z 400 (transient time 256 ms). Up to the top 10 most abundant isotope patterns with charge m/z 2 from the survey scan were selected with an isolation window of 1.6 Th and fragmented by HCD with normalized collision energies of 25. The maximum ion injection times for the survey scan and the MS/MS scans were 20 and 60 ms, respectively. The ion target value for both scan modes were set to 10^6. The dymamic exlusion was 25 s and 10 ppm. Muscle and liver fractions obtained in course of aldolase purification were analyzed in Orbitrap instruments as described previously.[16]

Data Analysis

The MS data was analyzed using MaxQuant[21] version 1.2.6.20. Proteins were identified by searching MS and MS/MS data of peptides against the UniProtKB/Swiss-Prot database. Carbamidomethylation of cysteines was set as a fixed modification. The initial search allowed mass deviation of the precursor ion was up to 6 ppm, and for the fragment masses, it was up to 20

DOI: 10.1021/acs.jproteome.5b00276
J. Proteome Res. 2015, 14, 3263−3273

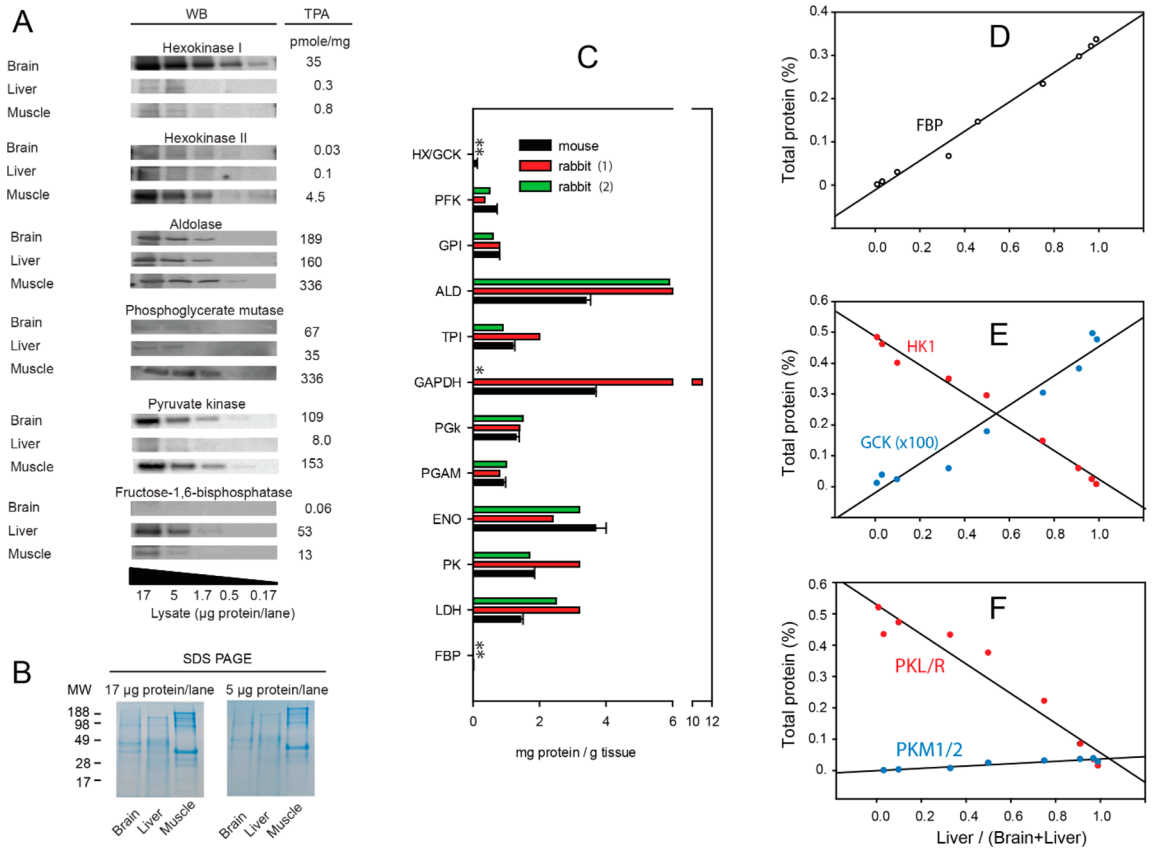

Figure 1. Validation of enzyme concentrations measured by TPA. (A) Quantitative Western blot analysis. Aliquots of tissue lysates used in the proteomic experiments (TPA-calculated concentration on the right) were separated by SDS-PAGE (B, Coomassie stained gels), blotted into nitrocellulose, and probed with antibodies against different glycolytic enzymes. (C) Comparison of the content of glycolytic enzymes in skeletal muscles of mouse (this study) and rabbit.[23,24] Asterisks indicate values missing in the cited studies. (D–F) Analysis of tissue mixtures. Whole cell lysates of mouse brain and liver were mixed in various ratios ranging from 1:99 to 99:1 and were analyzed as pure samples. The TPA analysis revealed a linear change of the abundance with respect to the mixing ratio. The linearity of the plots indicates direct proportionality of the protein concentrations in between the samples.

ppm. The maximum false peptide discovery rate was specified as 0.01. Protein concentrations were calculated on the basis of spectral protein intensity using the Total Protein Approach (TPA).[9]

RESULTS AND DISCUSSION

Proteomic Analysis

To measure concentration of enzymes involved in glycolysis and gluconeogenesis, we performed proteomic analyses of whole tissue lysates of mouse liver, brain and skeletal muscles using the MED FASP approach.[16] This method allows mapping at least 4000 proteins per sample in a relatively short mass spectrometer measuring time of 8 h.[22] This depth of proteome analysis was sufficient to identify all enzymes involved in the key metabolic processes such as glycolysis and gluconeogenesis. Notably, all proteins of these metabolic pathways were identified at high sequence coverage levels which allowed unequivocal distinction of majority of isoenzymes (Supporting Information Table 1). We calculated absolute levels of proteins by the "total protein approach" (TPA) method.[9] The values obtained for the individual glycolytic enzymes in 3 independent analyses showed on average 6.4% standard deviation (Supporting Information Table 1).

Although the TPA method has already been validated for several systems,[9,10] we tested the accuracy of the protein concentration calculations in several ways. First, we compared the TPA values with staining intensities in Western blot analysis (Figure 1A). We observed an excellent correlation between the Western blot data and the TPA values for most of the proteins. However, for those occurring at lower concentration, no reliable signal could be measured (for example, HK1 for liver and muscle, HK2 and PGAM for brain and liver). This reflects well-known limitations of the Western blot technique for quantitative analysis which is dependent on the antibody properties. Next, we compared the literature values of concentrations of glycolytic enzymes found in rabbit muscle[23,24] with our data on mouse skeletal muscle (Figure 1B). Despite comparison of different species, we observed almost identical content of the individual glycolytic/gluconeogenic enzymes in the muscles. In contrast to Scopes and Pette studies,[23,24] a recent proteomic study of Maughan et al. has revealed that rabbit skeletal muscles contained about three times higher concentrations of glycolytic enzymes than we observed in mouse muscles.[25] This discrepancy seems to reflect a different motoric behavior of the various mammalian species, differences in animal handling and sample preparation and, in the case of rabbit muscles, the use of animals from various providers. To test the linearity of the TPA concentrations of individual proteins as a function of the actual protein amount in the sample, we analyzed a series of mixtures of the whole tissue lysates of brain and liver (Supporting Information Table 2).

DOI: 10.1021/acs.jproteome.5b00276
J. Proteome Res. 2015, 14, 3263−3273

Since these tissues significantly differ in the content of several glycolytic/gluconeogenic enzymes, it was expected that the concentrations of these proteins would change proportionally to their average content in the mixture. Indeed, we observed a clear linear decrease or increase of the proteins as a function of liver-to-brain ratio (Figure 1C–E). Mixing liver and brain lysates to the ratio 1:100, we observed a 100-fold decrease of the fructose 1,6-bisphosphatase (FBP) content in comparison to the 100:1 mixture (Figure 1 C). Similar relations are shown for the hexokinase (HK1) glucokinase (GCK), and pyruvate kinase (PK) in the panels D and E (Figure 1). Finally, we tested the correlation between maximal activity (A_{max}) and the TPA-calculated concentration of an enzyme. For this purpose, we purified aldolases (ALDOA and ALDOB) from mouse liver and skeletal muscle (Figure 2A). At the subsequent steps of enzyme purification, fractions were analyzed using LC–MS/MS and the TPA method (Supporting Information Table 3), and were assayed for A_{max}. Plotting of the ALDO concentrations vs A_{max} revealed a direct proportionality of both values (Figure 2B). In the fractions of the highest enzyme enrichment, the content of ALDOA and B constituted 37 and 63% of total protein, respectively. Extrapolation of these to 100% of aldolase yielded for both proteins a concentration of 0.025 mmol/mg. This value is equal to the concentration expected for the pure proteins. Our experiment proved that TPA-based calculation results in accurate determination of protein concentrations.

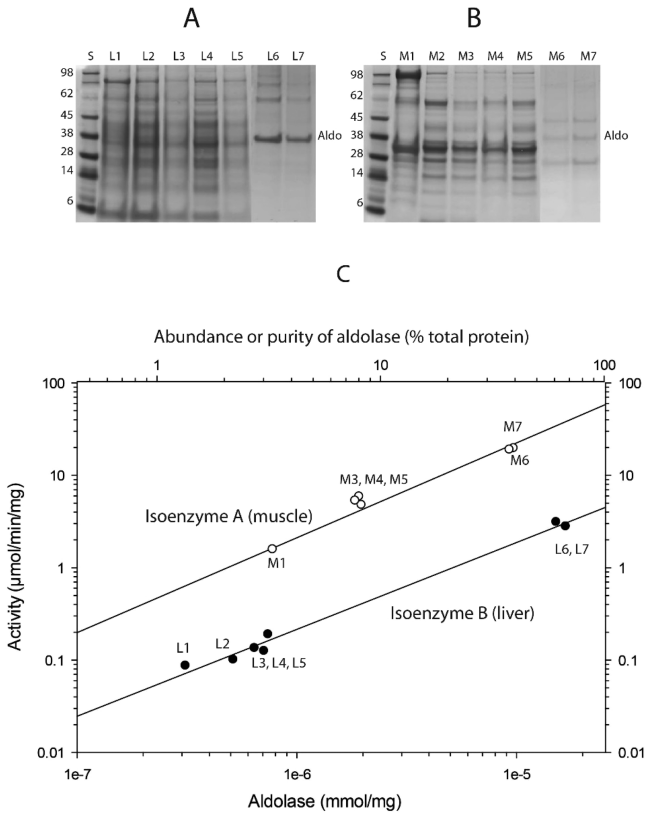

Figure 2. Correlation between the specific activity (biochemical assays) and protein abundance (mass spectrometry, TPA) of mouse aldolase A and B during the enzyme purification. Fractions at different steps of purification were assayed for the enzyme specific activities. Aliquots of the fractions were lysed in SDS-containing buffer (panels A and B) and, following FASP, were analyzed by LC–MS/MS. The obtained protein intensities were used for calculation of the protein content (%) and absolute concentrations (mmol/mg) in the fractions using the TPA approach.[9] L1-L7 and M1-M7 are the liver and muscle fractions, respectively.

Glycolysis versus Gluconeogensis

Energetic metabolism of skeletal muscles, liver and brain is among the most frequently studied fields of biomedicine (for comprehensive review see ref 26). Our TPA-based analysis of proteins concentration revealed significant differences in glucose metabolism-related enzymes between these tissues (Figure 3). This is in line with several previously published papers on the activity and expression of various glycolytic, gluconeogenic, and glycogen metabolism enzymes in muscles, brain and liver. As expected, the highest concentration of glycolytic enzymes was found in skeletal muscles. Compared to brain and liver, skeletal muscles also have the highest levels of the glycogen breakdown enzymes (PYG and PGM) and lactate dehydrogenase,[27] but relatively low content of hexokinases (HK). Clearly, phosphorylation of glucose is the main regulatory point of glycolysis in the muscles.

HK1 is a prevailing form of the kinase in almost all tested tissues, except skeletal muscles and liver, where HK2 and HK4 (glucokinase) predominates (Figure 5B). This is in line with older finding showing that HK1 is a basic enzyme enabling glucose estrification, and hence activation, in practically all tissues, while HK2 is expressed in insulin-dependent tissues, such as striated muscles and adipose tissue (for comprehensive review on metabolic and nonmetabolic functions of hexokinases see ref 28). The reversible, insulin-stimulated association of HK2 with mitochondria was hypothesized to be related to anabolic function of the isoform, e.g., to redirection of glucose molecule from glycolytic degradation to pentose phosphate pathway and/or glycogen synthesis.[29] It was also demonstrated that mitochondria-bound HK2 protects against apoptotic stimuli, whereas the cytosolic fraction of the isoform is involved in glucose deprivation-activated autophagy.[28] The low-affinity hexokinase isoform–glucokinase is expressed practically only in liver where it is a sole isoform of HK.

Liver, as opposed to skeletal muscles and brain, contains considerably high titers of gluconeogenic enzymes. The concentrations of FBP and pyruvate carboxylase (PC) in these organs are even higher than the levels of some of the glycolytic enzymes, e.g., PFK (Figure 3). This finding supports an old idea of the regulation of glycolysis by substrate cycle which might be formed between FBP and PFK.[30] The concept of the substrate cycle requires that the concentrations of both enzymes are of the same order. The concentration of FBP in liver is about 100 times higher than that of PFK. However, assuming that k_{cat} of PFK is over 20 times higher than that of FBP and that the activities of both the enzymes are reciprocally regulated by AMP and fructose-2,6-phoshate, it might be assumed that the substrate cycle does operate in liver.

To provide more general insight into the abundance of enzymes involved in glycolysis and gluconeogenesis, we reanalyzed proteomic data from additional 7 mouse organs, human cells and tissue, from our previous publications[10,11] (Supporting Information Tables S1, S4, and S5). Quantitative analysis of the data using TPA showed large differences, spanning several orders of magnitude, in the concentrations of the enzymes between the studied tissues and cells (Figure 4A). Most profound variations were found for FBP and HK ranging over 3–4 orders of magnitude, whereas abundances of other enzymes were almost within a 100-fold range, with the highest

DOI: 10.1021/acs.jproteome.5b00276
J. Proteome Res. 2015, 14, 3263–3273

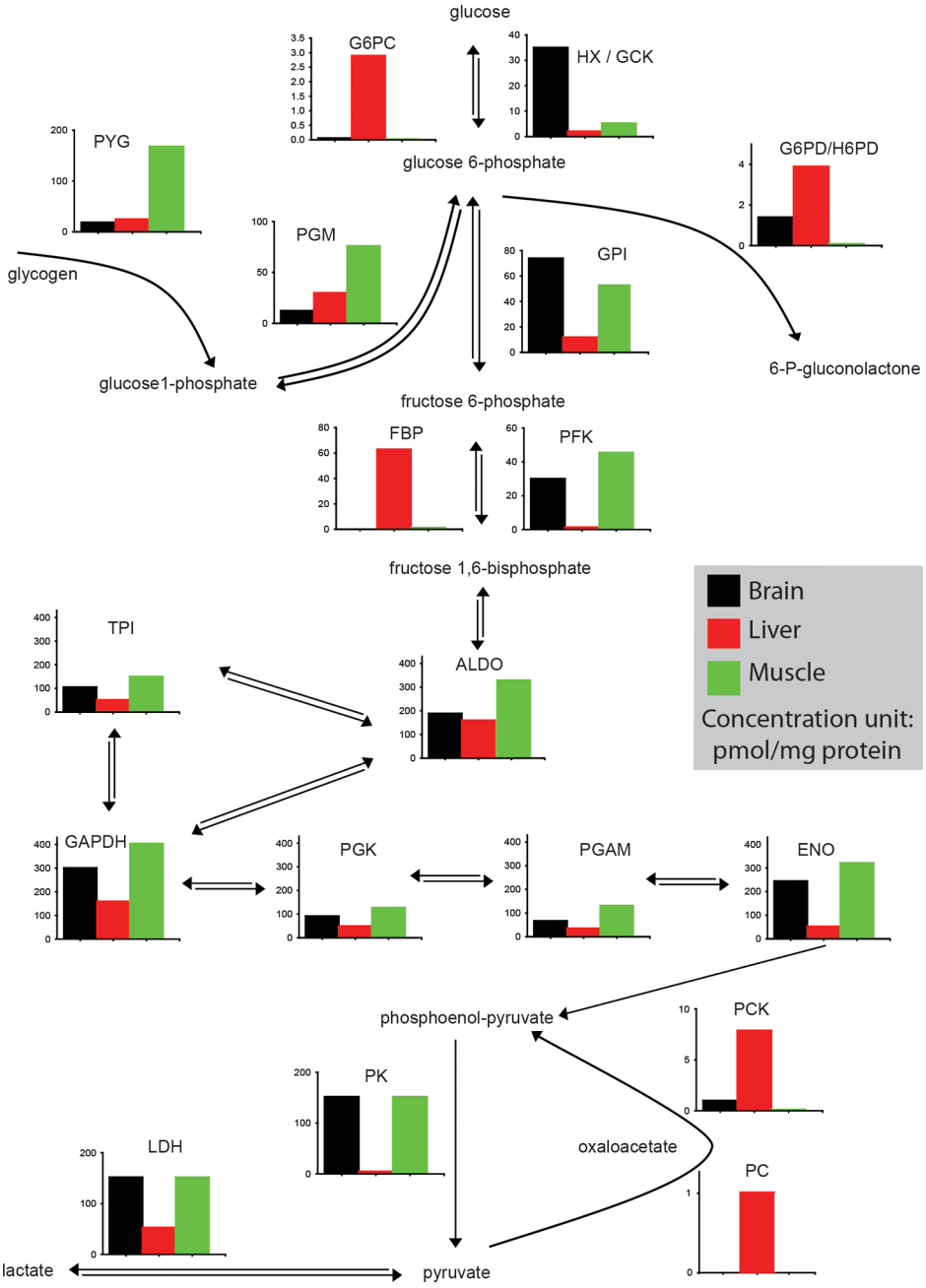

Figure 3. Abundances of proteins involved in the glycolytic/gluconeogenic pathway and selected members of the branching pathways. Concentration of a given enzyme is the sum of concentrations all its isoforms. The concentrations are calculated per subunit and are given in pmol/mg of total protein.

values in skeletal muscles and the lowest in lung and ovary tissue. In human cells, we found similar levels of the enzymes (Figure 4C). Interestingly, we observed a substantial increase of the FBP amount during CaCo-2 cells culture growth (Figure 4C). CaCo-2 cells are human epithelial colorectal adenocarcinoma cells which grow, differentiate and lose their neoplastic phenotype during their culture. This process resembles an inverted neoplastic transformation. Thus, this result suggests that, at least in some cancers (presumably those ones which develop in anaerobic environment within an organism), attenuation of the FBP titer may be related to more neoplastic phenotype.[31]

For a better comparison of individual enzyme profiles, we normalized the abundance values by dividing them by the median values of all glycolytic enzymes in each tissue (Figure 4C,D). This calculation clearly showed that in each tissue and cell, the levels of majority of the enzymes are similar. Usually, hexokinase/glucokinase, GPI and PFK are about 1 order of magnitude less abundant than other members of the pathway, from aldolase (ALDO) to LDH. Liver is the exception where PFK level is 2 orders of magnitude lower and pyruvate kinase (PK) is about 1 order of magnitude below the titers of other glycolytic enzymes. As a matter of fact, liver is the only organ where this classical profile of glycolysis/gluconeogenesis, with regard to the three regulatory enzymes—HK, PFK, and PK, exists. A very low amount of HK, which is over 100 times lower than the enzymes of triose phosphates metabolism, indicates that glucose is a substrate of little importance for liver.

DOI: 10.1021/acs.jproteome.5b00276
J. Proteome Res. 2015, 14, 3263−3273

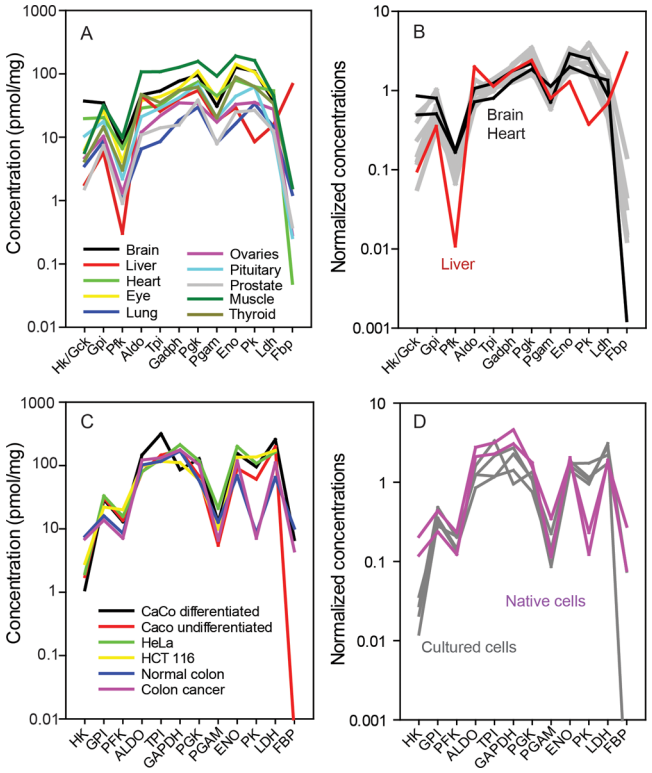

Figure 4. Survey of glycolytic enzyme titers across mouse organs (A and B) and native and cultured human cells (C and D) reveals discrete tissue-specific pathway profiles. (A and C) The titers of the individual enzymes are sum of titers of all their isoforms. (B and D) Normalized protein titers are calculated for each tissue by dividing the titers of enzymes (panels A and C) by their median value.

The highest variation in the protein concentrations among studied tissues and cells was observed in the case of HK and FBP. Brain and heart muscle have the highest concentrations of HK, whereas in skeletal muscles, this enzyme was 20- to 50-fold less abundant. Actually, brain and heart represent the second canonical glycolytic profile where all enzymes of the pathway are expressed practically at the same level (Figure 4B).

The concentration of FBP was highest in liver, which is known to be the major gluconeogenic organ in vertebrates. On the other hand, the lowest levels of FBP were found in brain and heart muscle. The foregoing observations enabled distinguishing of two major types of glycolytic/gluconeogenic pathway profiles in tissues. The "fast glucose uptake" profile exists in brain and heart muscle (Figure 4B, red lines), while the "gluconeogenesis rich" profile (Figure 4B, black lines), with the lowest levels of HK, PFK and PK, occurs in liver. In other mouse organs and human cells, we observed intermediate profiles (Figure 4B,D).

Cell-to-Cell Lactate Shuttle

The abundance of glycolytic enzymes in heart muscle is about 3-fold lower than that in skeletal muscle. On the other hand, heart, as opposed to skeletal muscle but similarly to brain, has the highest level of HK and abundance of this enzyme is similar to the concentrations of other glycolytic enzymes. This suggests that brain and heart cells utilize external glucose as a major source of energy. However, brain and heart are composed of two major types of cells: astrocytes and neurons, and cardiomyocytes and fibroblasts, respectively. It has been shown that even in the presence of glucose, both neurons and cardiomiocytes preferentially utilize lactate and, hence, are highly sensitive to hypoxia.[32−34] It has also been shown that astrocytes take up the majority of the brain glucose and oxidize it to lactate which is then transported to neurons and oxidized in the Krebs cycle. Thus, the similarities in the heart and brain glycolytic profiles, and in their physiological response to hypoxia, may suggest that the classical cell-to-cell lactate shuttle operates also in heart where, presumably, fibroblasts may deliver lactate to cardiomyocytes.

Glycolytic Complex

Our study demonstrates that in most cases, all glycolytic enzymes are present at similar titers within a tissue or cell line and that the amount of triose phosphates metabolism enzymes is about 2-fold higher than those of hexoses metabolism. The capacities of individual glycolytic enzymes to catalyze their reactions differ significantly because of their quite different kinetic properties. Thus, the observed similarity of concentrations of these enzymes is unexpected and raises a question about its physiological function.

Over the past decade, it has been demonstrated that, at least in some tissues, glycolytic enzymes may form macromolecular complexes, and that disruption of such complexes leads to inhibition of glycolysis and energy production in striated

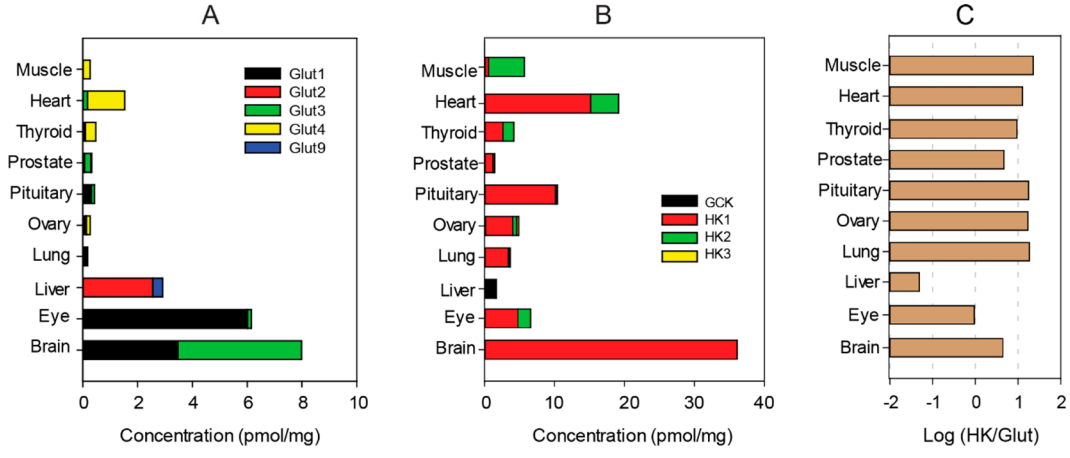

Figure 5. Occurrence and levels of glucose transporters (GLUT). (A) Concentrations of glucose transporters in mouse tissues. (B) Titers of hexokinases in mouse tissues. (C) Abundance of the glucose transporters relatively to hexokinase.

DOI: 10.1021/acs.jproteome.5b00276
J. Proteome Res. 2015, 14, 3263−3273

muscles[35] and in some cancer cell lines,[36] whereas the activities of the individual enzymes remain unaffected. The stoichiometry of the glycolytic complex is unknown, but it is reasonable to assume that the enzymes which associate together to work as the glycolytic machinery should be present in a cell in a similar abundance. This is exactly what we found in mouse tissues (with the exception of liver) and cancer cells. As a matter of fact, even in liver the concentrations of enzymes involved in triose phosphates metabolism, from ALDO to enolase, are at very similar levels, supporting the hypothesis that the macromolecular organization of the pathway is not an exception but rather the universal mode in which glycolysis operates.

Tissue-Specific Localization of Glucose Transporters

The passage of glucose through the plasma membrane is facilitated by glucose transporters known as Glut- or Slc2-family transporters. Our results confirm the tissue-specific expression of these transporters. Whereas Glut1 and Glut3 are highly abundant in brain, Glut2 and Glut9 are restricted to liver, and Glut4 is ubiquitously expressed in all types of muscles (Figure 5A). We found that in liver, the ratio of the amount of Glut to HK is high and that in brain, these proteins have similar titers (Figure 5B). On the other hand, in muscles and some other organs, abundance of the transporter (mainly Glut4) is approximately 10 times lower than that of HK (Figure 5B). Considering that k_{cat} of the glucose transporter is about 10-fold higher than k_{cat} of HK, these observations reflect a fine-tuning of these two proteins.

Energy Metabolism Landscape

Generation of large-scale data sets followed by the label-free analysis of protein abundances allows system-wide insight into organization and relations between varieties of cellular processes. Our data on 10 mouse organs covers more than 10 000 proteins. Of those, proteins directly involved in carbohydrate metabolism and in energy production are comprehensively represented at high sequence coverage. This tempted us to compare the contribution of these processes to overall energy metabolism in the mouse organs. Figure 6 shows concentrations of key proteins involved in glycolysis, tricarboxylic acid cycle, pentose phosphate pathway (PPP), oxidative phosphorylation (OxPhos) and free fatty acids (FFA) metabolism (FFAM). To achieve this, we calculated relative pathway abundances (Figure 7) in the tissues.

The calculations revealed that in skeletal muscles, where the highest abundance of glycolytic enzymes was observed, both TCA and OxPhos pathways were also overrepresented, while the PPP and FFAM levels were the lowest. The positive correlation between glycolysis, and TCA and OxPhos level, and the inverse correlation between glycolysis, and gluconeogenesis and PPP pathways was observed in all the tested organs.

In contrast to other highly glycolytic organs such as skeletal muscle and brain, the mouse heart contained very high amount of FFA enzymes, accompanied by the highest abundance of TCA and OxPhos proteins of all studied tissues. This indicates that FFA are one of the favorable energetic substrates for heart. Although we found even higher capacity to metabolize FFA in liver, it did not correlate with very high TCA and OxPhos. Clearly, in contrast to heart muscle, in liver, FFA are not used for energy generation.

On the basis of the quantitative proteomic data, two profiles of cellular energy metabolism might be distinguished: the "energy-dissipating" profile which operates in muscles and brain, and the "anabolic-like" system, which may be characterized by low capacity to ATP synthesis and relatively high abundance of the PPP enzymes.

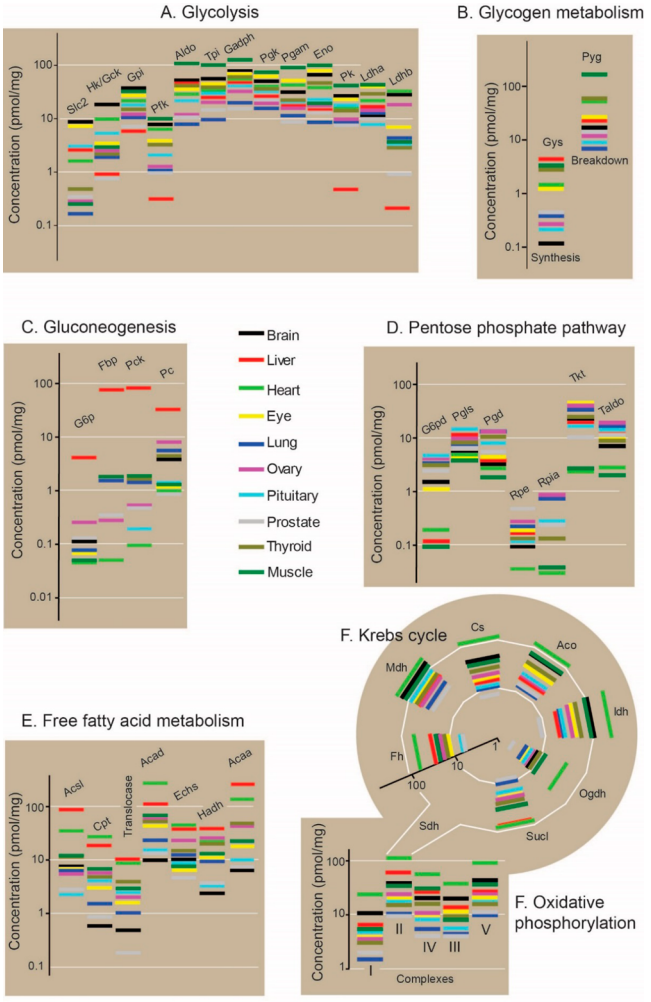

Figure 6. Concentrations of major enzymes involved in energy metabolism. (A) Glycolysis, (B) glycogen metabolism, (C) gluconeogenesis, (D) pentose phosphate pathway, (E) free fatty acid degradation, (F) Krebs cycle, and (G) oxidative phosphorylation. In A–F, the concentrations represent the sum of all isoforms for each enzyme. In G, median concentrations of all components of individual complexes are shown. Concentrations of the glycolytic enzymes are calculated with respect to their quaternary structure compositions: tetrameric for Pfk, Aldo, Gadph, Pk, Ldh, and dimeric for Gpi, Tpi, Pgam, Eno.

Unexpectedly, tissues belonging to the first system possess a lower amount of PPP enzymes despite their high capacity to produce reactive oxygen species. It is well-known that thioredoxin and glutathione redox systems which use the PPP-derived NADPH are crucial for antioxidant defense.[37] Thus, the source of NADPH for anti-ROS defense in muscle tissue remains unclear.

No Evidence for Extensive Lysine Acetylation in Glycolytic Enzymes in Normal Tissue

Several recent studies have emphasized the role of lysine acetylation in metabolism regulation including glycolysis and gluconeogenesis.[2,3,38−40] The evidence provided is based on analysis of peptides that were affinity-enriched using antiacetyl-lysine antibodies and the changes in the acetylation were

DOI: 10.1021/acs.jproteome.5b00276
J. Proteome Res. 2015, 14, 3263−3273

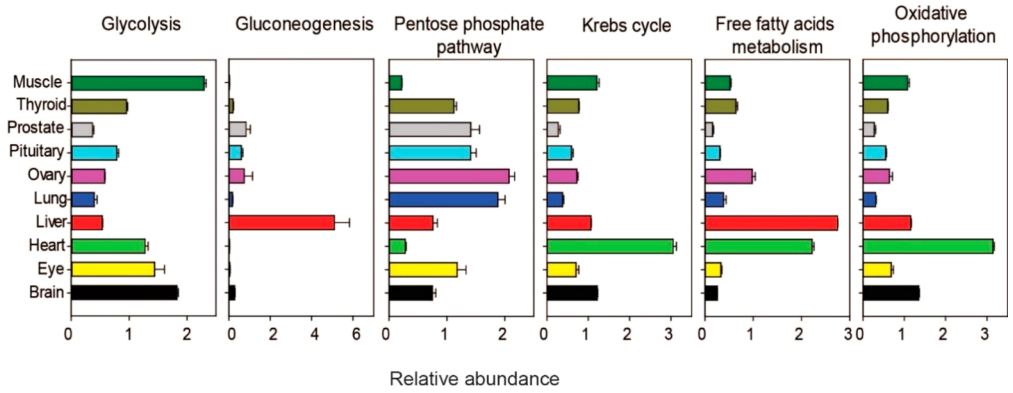

Figure 7. Relative abundances of energy metabolism pathways in mouse organs. Relative abundances of pathways are the average of organ-normalized titers of enzymes involved in each of the pathway. The values were calculated using the titers of the enzymes selected in Figure 6.

monitored by Western blotting technique. Alternatively, changes in abundances of the acetylated peptides were also demonstrated using SILAC[39] or iTRAQ-labeling.[40] All these techniques allow only relative comparisons and do not provide the essential information on the acetyl-occupancy of the analyzed sites. To provide insights in the extent of acetylation of glycolytic enzymes, we searched our spectra for this modification in mouse tissues (Supporting Information Table 6). Our analysis enabled identification of 372 acetylated peptides in 234 mouse proteins. The largest numbers of acetylation sites were found in nuclear (35%) and mitochondrial (18%) proteins. The most prominent sites are the well-documented acetylation sites on core histones H4 and H3. We found large number of lysine-acetylated sites in enzymes involved in lipid metabolism or oxidative phosphorylation, but we did not find any acetylated site in proteins of the glycolytic pathway. Our data suggests that if the previously observed acetylation is a general phenomenon, then it occurs only at very low protein fraction and, therefore, escaped from detection in our screen. In conclusion, it seems unlikely that this type of modification regulates directly any of the steps in glycolysis or gluconeogenesis. However, it cannot be excluded that lysine acetylated glycolytic enzymes modulate the rate of glycolytic/gluconeogenic flux acting as a regulators of transcription, translation and/or affecting the activity of other regulatory proteins. In contrast to lysine acetylation, we observed phosphorylation of serine and threonine residues in PFK, ALDO, glyceraldehyde dehydrogenase (GADPH), phosphoglyceromutase (PGAM) of the glycolytic pathway and in glycogen breakdown branch at PYG and PGM (Supporting Information Table 6). Most of the sites were already found in large-scale phosphoproteomic analysis of mouse tissues.[41] Notably, we observed some of the modifications at high site occupancy (ratio of phosphorylated site to nonmodified site), which indicates their potential role for regulation of the glycolytic flux.

Cytosolic Fractions Contain Only a Portion of Glycolytic Enzymes

All glycolytic enzymes are commonly considered as freely soluble cytoplasmic proteins, and therefore, it is a routine to extract them from tissues in the absence of chaotropic reagents such as detergents or urea, which is also prerequisite for kinetic studies and characterization of the enzymes by biochemical methods. We compared the concentrations of the enzymes in the whole lysates with those in the cytosolic fraction (Supporting Information Table 7) (Figure 8A). On average,

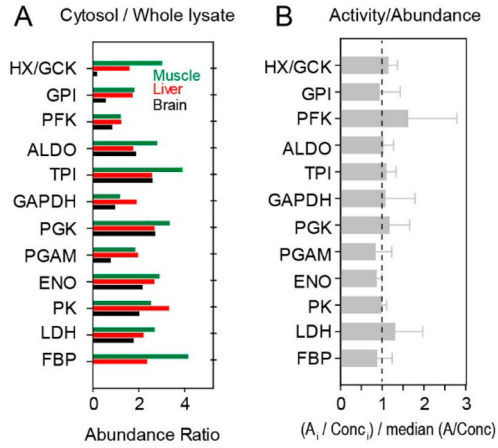

Figure 8. The level of extraction of glycolytic enzymes from tissues and catalytic potential of the enzymes. (A) Enrichment of the enzymes in cytosolic fractions. (B) Total activities correlate with protein abundances.

the glycolytic enzymes were enriched 2.3-fold in the cytosol. However, some of the enzymes, such as HK and GPI in brain and PFK in all tested tissues, were not enriched in this fraction which suggests that the large portion of the protein was in the insoluble protein fraction. Because activity of enzymes is commonly assayed in cytosolic extracts, this observation indicates that some conclusions drawn solely on the basis of kinetic data can be very inaccurate.

Correlation between Protein Abundance and Enzymatic Activity

In a biological system, metabolic capacity of enzymes is defined by their abundance and kinetic properties. At substrate concentrations exceeding several-fold Michaelis–Menten constant, the maximal activity A_{max}, which is close to V_{max}, is the kinetic measure of the impact of an enzyme on a given process. To extend the proteomic picture of the glycolytic/gluconeogenic pathway by a kinetic component, we measured A_{max} for all 11 glycolytic enzymes and FBP in cytosolic fractions of brain, liver, and skeletal muscles (Supporting Information Table 8). Comparison of the A_{max} values with the enzyme concentrations revealed high degree of correlation (Figure 8B). This suggests that enzyme concentrations provide a good approximation of the relative activities. We observed similar abundance/activity correlation between slow and fast twitch muscle fibers.[27]

DOI: 10.1021/acs.jproteome.5b00276
J. Proteome Res. 2015, 14, 3263−3273

Table 1. k_{cat} Values of the Glycolytic Enzymes and FBP

	k_{cat} (s^{-1})*			dominant isoform		
enzyme	brain	liver	muscle	brain	liver	muscle
HK/GCK	79	110	79	I(94%)	IV(95%),	II(97%)
GPI	2,200	3,100	870			
PFK	750	2,200	640	m(39%)	l(62%)	m(99%)
ALD	27	20	34	A(70%)	B(92%)	A(99%)
TPI	68	50	44			
GAPDH	140	55	260			
PGK	114	196	87			
PGAM	115	310	350	1	1	2
ENO	15	17	20	γ(48%)/ α(49%)	α(87%)	β(95%)
PK	590	640	490	M	R/L	M
LDH	410	1,000	490	b	a	a/b
FBP	76	88	34	n.d.	1	2

*The k_{cat} values were calculated by dividing A_{max} values by the enzyme concentrations obtained from the analysis of cytosolic fractions (Supporting Information Table 7).

Catalytic Constants Can Be Determined in Crude Lysates

Dividing the A_{max} values by the enzyme concentrations, we calculated the catalytic constants of the enzymes, k_{cat} (Table 1). This value represents the number of reactions catalyzed by an enzyme during a time unit. In most cases, the k_{cat} values of a given enzyme varied 22 to 3-fold among the tissues. These differences may reflect occurrence of various isoenzymes (Table 1) differing in their catalytic properties, quaternary structures, as well as post-translational modifications that modulate enzymatic activity.

In the studied tissues, the highest k_{cat} values were found for GPI, PFK, PK and LDH, and they were often about 1 order of magnitude higher than for the rest of the enzymes of glycolytic pathway. The majority of the k_{cat} values were in the wide range of those determined for purified enzymes (BRENDA database, http://www.brenda-enzymes.org/). Until now, determination of k_{cat}, the fundamental kinetic parameter, required purification of enzymes prior to kinetic measurements. Since the purification is usually time-consuming and laborious, the k_{cat} values have been determined only for a limited number of enzymes, mostly in nonmodel organisms. Here, we demonstrated that k_{cat} can be estimated from parallel determination of maximal activity in a complex mixture and the proteomic experiment.

CONCLUSIONS

Glycolysis is one of a key metabolic processes in all organisms. In this work, we showed that glycolysis can be comprehensively studied by integrating proteomics and enzyme kinetics. Importantly, we showed that proteomic profiling is a good proxy for studying metabolic potential of glycolytic enzymes. We demonstrated that in contrast to classical methods requiring enzyme purification, enzyme k_{cat} values can be determined directly in a cell lysate. Such data can be valuable information, useful in metabolic modeling approaches.[42]

Additionally, our data revealed existence of two basic profiles of glycolysis. The "fast glucose" uptake profile is characteristic for brain and heart muscle, whereas the "gluconeogenic rich" profile is typical for liver. We demonstrated that the maximal enzymatic activity of hexokinase is almost always 10−100 times lower than the activities of other glycolytic enzymes. This highlights the essential role of HK in regulation of glycolysis in all the tested tissues and cell lines, except heart and brain. Unexpectedly, the generally accepted model of glycolysis regulation triggered by PFK and PK appeared to be typical only for liver.

Finally, despite extensive proteomic analysis, we were unable to detect lysine acetylated glycolytic enzymes in brain, liver, and skeletal muscles, which diminishes the potential role of this post-translational modification in a direct regulation of glycolysis.

ASSOCIATED CONTENT

Supporting Information

Supporting Information (SI) Table 1, analysis of mouse tissue lysates; SI Table 2, analysis of brain and liver lysate mixtures; SI Table 3, analysis of protein fractions obtained during purification of aldolase from liver and muscle extracts; SI Table 4, analysis of colon and colon cancer samples; SI Table 5, analysis of Caco-2 (undifferentiated and differentiated), HeLa and HCT116 cells; SI Table 6, identification of acetylation and phosphorylation sites; SI Table 7, analysis of protein extracts used for determination of enzymatic activities; SI Table 8, determination of enzymatic activities. The Supporting Information is available free of charge on the ACS Publications website at DOI: 10.1021/acs.jproteome.5b00276. The mass spectrometry proteomics data form mouse brain, liver and skeletal muscle have been deposited to the ProteomeXchange Consortium[43] via the PRIDE partner repository with the data set identifier PXD002156.

AUTHOR INFORMATION

Corresponding Author

*Address: Biochemical Proteomics Group, Department of Proteomics and Signal Transduction, Max-Planck-Institute of Biochemistry, Am Klopferspitz 18, D-82152 Martinsried, Germany. Tel.: +49 89 8578 2205. E-mail: jwisniew@biochem.mpg.de.

Notes

The authors declare no competing financial interest.

ACKNOWLEDGMENTS

We thank Katharina Zettl for technical assistance, Igor Paron and Korbinian Mayr for support in mass spectrometric analysis, and Dr. Atul Deshmukh for critical discussion. This work was

DOI: 10.1021/acs.jproteome.5b00276
J. Proteome Res. 2015, 14, 3263−3273

supported by the Max-Planck Society for the Advancement of Science and the Polish National Center of Science (DEC-2011/01/N/NZ5/04253) and Polish Ministry of Science and Higher Education (Contract Grant Number: N N401 376139).

REFERENCES

(1) Boiteux, A.; Hess, B. Design of glycolysis. *Philos. Trans. R. Soc., B* **1981**, *293* (1063), 5−22.

(2) Hallows, W. C.; Yu, W.; Denu, J. M. Regulation of glycolytic enzyme phosphoglycerate mutase-1 by Sirt1 protein-mediated deacetylation. *J. Biol. Chem.* **2012**, *287* (6), 3850−8.

(3) Lv, L.; Li, D.; Zhao, D.; Lin, R.; Chu, Y.; Zhang, H.; Zha, Z.; Liu, Y.; Li, Z.; Xu, Y.; Wang, G.; Huang, Y.; Xiong, Y.; Guan, K. L.; Lei, Q. Y. Acetylation targets the M2 isoform of pyruvate kinase for degradation through chaperone-mediated autophagy and promotes tumor growth. *Mol. Cell* **2011**, *42* (6), 719−30.

(4) Spoden, G. A.; Rostek, U.; Lechner, S.; Mitterberger, M.; Mazurek, S.; Zwerschke, W. Pyruvate kinase isoenzyme M2 is a glycolytic sensor differentially regulating cell proliferation, cell size and apoptotic cell death dependent on glucose supply. *Exp. Cell Res.* **2009**, *315* (16), 2765−74.

(5) Vander Heiden, M. G.; Locasale, J. W.; Swanson, K. D.; Sharfi, H.; Heffron, G. J.; Amador-Noguez, D.; Christofk, H. R.; Wagner, G.; Rabinowitz, J. D.; Asara, J. M.; Cantley, L. C. Evidence for an alternative glycolytic pathway in rapidly proliferating cells. *Science* **2010**, *329* (5998), 1492−9.

(6) Costenoble, R.; Picotti, P.; Reiter, L.; Stallmach, R.; Heinemann, M.; Sauer, U.; Aebersold, R. Comprehensive quantitative analysis of central carbon and amino-acid metabolism in Saccharomyces cerevisiae under multiple conditions by targeted proteomics. *Mol. Syst. Biol.* **2011**, *7*, 464.

(7) Drabovich, A. P.; Pavlou, M. P.; Dimitromanolakis, A.; Diamandis, E. P. Quantitative analysis of energy metabolic pathways in mcf-7 breast cancer cells by selected reaction monitoring assay. *Mol. Cell. Proteomics* **2012**, *11* (8), 422−34.

(8) Murphy, J. P.; Pinto, D. M. Targeted proteomic analysis of glycolysis in cancer cells. *J. Proteome Res.* **2011**, *10* (2), 604−13.

(9) Wisniewski, J. R.; Rakus, D. Multi-enzyme digestion FASP and the 'Total Protein Approach'-based absolute quantification of the Escherichia coli proteome. *J. Proteomics* **2014**, *109*, 322−31.

(10) Wisniewski, J. R.; Hein, M. Y.; Cox, J.; Mann, M. A "proteomic ruler" for protein copy number and concentration estimation without spike-in standards. *Mol. Cell. Proteomics* **2014**, *13* (12), 3497−506.

(11) Wisniewski, J. R.; Ostasiewicz, P.; Dus, K.; Zielinska, D. F.; Gnad, F.; Mann, M. Extensive quantitative remodeling of the proteome between normal colon tissue and adenocarcinoma. *Mol. Syst. Biol.* **2012**, *8*, 611.

(12) Teusink, B.; Passarge, J.; Reijenga, C. A.; Esgalhado, E.; van der Weijden, C. C.; Schepper, M.; Walsh, M. C.; Bakker, B. M.; van Dam, K.; Westerhoff, H. V.; Snoep, J. L. Can yeast glycolysis be understood in terms of in vitro kinetics of the constituent enzymes? Testing biochemistry. *Eur. J. Biochem.* **2000**, *267* (17), 5313−29.

(13) Vildhede, A.; Karlgren, M.; Svedberg, E. K.; Wisniewski, J. R.; Lai, Y.; Noren, A.; Artursson, P. Hepatic uptake of atorvastatin: influence of variability in transporter expression on uptake clearance and drug-drug interactions. *Drug Metab. Dispos.* **2014**, *42* (7), 1210−8.

(14) Penhoet, E. E.; Kochman, M.; Rutter, W. J. Iosolation of fructose diphosphate aldolases A, B, and C. *Biochemistry* **1969**, *8* (11), 4391−5.

(15) Wisniewski, J. R.; Zielinska, D. F.; Mann, M. Comparison of ultrafiltration units for proteomic and N-glycoproteomic analysis by the filter-aided sample preparation method. *Anal. Biochem.* **2011**, *410* (2), 307−9.

(16) Wisniewski, J. R.; Mann, M. Consecutive proteolytic digestion in an enzyme reactor increases depth of proteomic and phosphoproteomic analysis. *Anal. Chem.* **2012**, *84* (6), 2631−7.

(17) Wisniewski, J. R.; Gaugaz, F. Z. Fast and sensitive total protein and peptide assays for proteomic analysis. *Anal. Chem.* **2015**, *87*, 4110−6.

(18) Ziolkowski, P.; Gamian, E.; Osiecka, B.; Zougman, A.; Wisniewski, J. R. Immunohistochemical and proteomic evaluation of nuclear ubiquitous casein and cyclin-dependent kinases substrate in invasive ductal carcinoma of the breast. *J. Biomed. Biotechnol.* **2009**, *2009*, 919645.

(19) Gizak, A.; Dzugaj, A. FBPase is in the nuclei of cardiomyocytes. *FEBS Lett.* **2003**, *539* (1−3), 51−5.

(20) Wisniewski, J. R.; Dus, K.; Mann, M. Proteomic workflow for analysis of archival formalin-fixed and paraffin-embedded clinical samples to a depth of 10 000 proteins. *Proteomics: Clin. Appl.* **2013**, *7* (3−4), 225−33.

(21) Cox, J.; Mann, M. MaxQuant enables high peptide identification rates, individualized p.p.b.-range mass accuracies and proteome-wide protein quantification. *Nat. Biotechnol.* **2008**, *26* (12), 1367−72.

(22) Wisniewski, J. R.; Koepsell, H.; Gizak, A.; Rakus, D. Absolute protein quantification allows differentiation of cell-specific metabolic routes and functions. *Proteomics* **2015**, *14*, 353−65.

(23) Scopes, R. K. Studies with a reconstituted muscle glycolytic system. The rate and extent of creatine phosphorylation by anaerobic glycolysis. *Biochem. J.* **1973**, *134* (1), 197−208.

(24) Pette, D. Some aspects of supramolecular organization of glycogenolytic and glycolytic enzymes in muscle. *Acta Histochem. Suppl.* **1975**, *14*, 47−68.

(25) Maughan, D. W.; Henkin, J. A.; Vigoreaux, J. O. Concentrations of glycolytic enzymes and other cytosolic proteins in the diffusible fraction of a vertebrate muscle proteome. *Mol. Cell. Proteomics* **2005**, *4*, 1541−9.

(26) Ohlendieck, K. Proteomics of skeletal muscle glycolysis. *Biochim. Biophys. Acta* **2010**, *1804*, 2089−2101.

(27) Rakus, D.; Gizak, A.; Deshmukh, A.; Wisniewski, J. R. Absolute quantitative profiling of the key metabolic pathways in slow and fast skeletal muscle. *J. Proteome Res.* **2015**, *14* (3), 1400−11.

(28) Roberts, D. J.; Miyamoto, S. Hexokinase II integrates energy metabolism and cellular protection: Akting on mitochondria and TORCing to autophagy. *Cell Death Differ.* **2015**, *22*, 364.

(29) Wilson, J. E. Isozymes of mammalian hexokinase: structure, subcellular localization and metabolic function. *J. Exp. Biol.* **2003**, *206*, 2049−57.

(30) Challiss, R. A.; Arch, J. R.; Crabtree, B.; Newsholme, E. A. Measurement of the rate of substrate cycling between fructose 6-phosphate and fructose 1,6-bisphosphate in skeletal muscle by using a single-isotope technique. *Biochem. J.* **1984**, *223* (3), 849−53.

(31) Dong, C.; Yuan, T.; Wu, Y.; Wang, Y.; Fan, T. W.; Miriyala, S.; Lin, Y.; Yao, J.; Shi, J.; Kang, T.; Lorkiewicz, P.; Clair, D., St; Hung, M. C.; Evers, B. M.; Zhou, B. P. Loss of FBP1 by Snail-mediated repression provides metabolic advantages in basal-like breast cancer. *Cancer Cell* **2013**, *23* (3), 316−31.

(32) Belanger, M.; Allaman, I.; Magistretti, P. J. Brain energy metabolism: focus on astrocyte-neuron metabolic cooperation. *Cell Metab.* **2011**, *14* (6), 724−38.

(33) Brooks, G. A. Cell-cell and intracellular lactate shuttles. *J. Physiol.* **2009**, *587* (Pt 23), 5591−600.

(34) Jugdutt, B. I. Ventricular remodeling after infarction and the extracellular collagen matrix: when is enough enough? *Circulation* **2003**, *108* (11), 1395−403.

(35) Wojtas, K.; Slepecky, N.; von Kalm, L.; Sullivan, D. Flight muscle function in Drosophila requires colocalization of glycolytic enzymes. *Mol. Biol. Cell* **1997**, *8* (9), 1665−75.

(36) Kowalski, W.; Nocon, D.; Gamian, A.; Kolodziej, J.; Rakus, D. Association of C-terminal region of phosphoglycerate mutase with glycolytic complex regulates energy production in cancer cells. *J. Cell. Physiol.* **2012**, *227* (6), 2613−21.

(37) Reid, M. B. Free radicals and muscle fatigue: Of ROS, canaries, and the IOC. *Free Radical Biol. Med.* **2008**, *44* (2), 169−79.

(38) Kim, S. C.; Sprung, R.; Chen, Y.; Xu, Y.; Ball, H.; Pei, J.; Cheng, T.; Kho, Y.; Xiao, H.; Xiao, L.; Grishin, N. V.; White, M.; Yang, X. J.; Zhao, Y. Substrate and functional diversity of lysine acetylation revealed by a proteomics survey. *Mol. Cell* **2006**, *23* (4), 607−18.

DOI: 10.1021/acs.jproteome.5b00276
J. Proteome Res. 2015, 14, 3263−3273

(39) Wang, Q.; Zhang, Y.; Yang, C.; Xiong, H.; Lin, Y.; Yao, J.; Li, H.; Xie, L.; Zhao, W.; Yao, Y.; Ning, Z. B.; Zeng, R.; Xiong, Y.; Guan, K. L.; Zhao, S.; Zhao, G. P. Acetylation of metabolic enzymes coordinates carbon source utilization and metabolic flux. *Science* **2010**, *327* (5968), 1004−7.
(40) Zhao, S.; Xu, W.; Jiang, W.; Yu, W.; Lin, Y.; Zhang, T.; Yao, J.; Zhou, L.; Zeng, Y.; Li, H.; Li, Y.; Shi, J.; An, W.; Hancock, S. M.; He, F.; Qin, L.; Chin, J.; Yang, P.; Chen, X.; Lei, Q.; Xiong, Y.; Guan, K. L. Regulation of cellular metabolism by protein lysine acetylation. *Science* **2010**, *327* (5968), 1000−4.
(41) Huttlin, E. L.; Jedrychowski, M. P.; Elias, J. E.; Goswami, T.; Rad, R.; Beausoleil, S. A.; Villen, J.; Haas, W.; Sowa, M. E.; Gygi, S. P. A tissue-specific atlas of mouse protein phosphorylation and expression. *Cell* **2010**, *143* (7), 1174−89.
(42) Matsson, P.; Fenu, L. A.; Lundquist, P.; Wisniewski, J. R.; Kansy, M.; Artursson, P. Quantifying the impact of transporters on cellular drug permeability. *Trends Pharmacol. Sci.* **2015**, *36* (5), 255−62.
(43) Vizcaino, J. A.; Cote, R. G.; Csordas, A.; Dianes, J. A.; Fabregat, A.; Foster, J. M.; Griss, J.; Alpi, E.; Birim, M.; Contell, J.; O'Kelly, G.; Schoenegger, A.; Ovelleiro, D.; Perez-Riverol, Y.; Reisinger, F.; Rios, D.; Wang, R.; Hermjakob, H. The PRoteomics IDEntifications (PRIDE) database and associated tools: status in 2013. *Nucleic Acids Res.* **2013**, *41*, D1063−9.

DOI: 10.1021/acs.jproteome.5b00276
J. Proteome Res. 2015, 14, 3263−3273